Statistical theory of shot noise in quasi-one-dimensional field-effect transistors in the presence of electron-electron interaction

Alessandro Betti, Gianluca Fiori, and Giuseppe Iannaccone
Dipartimento di Ingegneria dell'Informazione: Elettronica, Informatica, Telecomunicazioni, Università di Pisa, Via Caruso 16, 56122 Pisa, Italy

(Received 27 April 2009; revised manuscript received 19 October 2009; published 21 January 2010)

We present an expression for the shot noise power spectral density in quasi-one dimensional conductors electrostatically controlled by a gate electrode, which includes the effects of Coulomb interaction and of Pauli exclusion among charge carriers. In this sense, our expression extends the well known Landauer-Büttiker noise formula to include the effect of Coulomb interaction inducing fluctuations of the potential in the device region. Our approach is based on evaluating the statistical properties of the scattering matrix and on a second-quantization many-body description. From a quantitative point of view, statistical properties are obtained by means of Monte Carlo simulations on an ensemble of different configurations of injected states, requiring the solution of the Poisson-Schrödinger equation on a three-dimensional grid, with the nonequilibrium Green's functions formalism. In a series of examples, we show that failure to consider the effects of Coulomb interaction on noise leads to a gross overestimation of the noise spectrum of quasi-one-dimensional devices.

DOI: 10.1103/PhysRevB.81.035329 PACS number(s): 73.50.Td, 73.63.Nm

I. INTRODUCTION

As quasi-one-dimensional field-effect transistors (FETs), based for example on Carbon nanotubes (CNTs) or Silicon nanowires (SNWs), are increasingly investigated as a possible replacement for conventional planar FETs, it is important to achieve complete understanding of the properties of shot noise of one-dimensional conductors electrostatically controlled by a third (gate) electrode. Shot noise is particularly sensitive to carrier-carrier interaction, which in turn can be particularly significant in one-dimensional nanoscale conductors, where electrons are few and screening is limited.[1] Low-frequency $1/f$ noise in quasi one-dimensional conductors has been the subject of interest for several authors,[2–4] whereas few experimental papers on shot noise have recently been published.[5,6]

Due to the small amount of mobile charge in nanoscale one-dimensional FETs, even in strong inversion, drain current fluctuations can heavily affect device electrical behavior. Of course, noise is an unavoidable and undesirable feature of electron devices, and its effect must be minimized or kept within tolerable levels for the operation of electronic circuits. From a more fundamental point of view, it is also a rich source of information on electron-electron interaction, which cannot be obtained from dc or ac electrical characteristics.

The main sources of noise are injection from the contacts into the device region, through the random occupation of states around the Fermi energy at the contacts, and partial transmission of electrons through the conductor, which gives rise to the so-called partition noise. The main types of interaction that have a clear effect on noise are Pauli exclusion, which reduces fluctuations of the rate of injected electrons by limiting the occupancy of injected states, and Coulomb repulsions among electrons, which is the cause of fluctuations of the potential in the device region, that often suppress, but sometimes enhance the effect of fluctuations in the rate of injected electrons.

The combined effect of Pauli exclusion and Coulomb repulsion on shot noise has been investigated in the case of ballistic double gate MOSFETs,[7] in planar MOSFETs[8] and in resonant tunneling diodes.[9–11] There are still few attempts[12] to a complete quantitative understanding of shot noise in ballistic CNT and SNW-FETs. Indeed, when addressing a resonant tunneling diode one can usually adopt an approach that exploits the fact that the two opaque barriers break the device in three loosely coupled regions (the two contacts and the well), among which transitions can described by Fermi golden rule, as has been done in Refs. 9–11. This is not possible in the case of a transistor, where coupling between the channel and the contacts is very good.

Another important issue is represented by the fact that the widely known Landauer-Büttiker's noise formula,[13,14] does not take into account the effect of Coulomb interaction on shot noise through potential fluctuations. Indeed, recent experiments on shot noise in CNT-based Fabry Perot interferometers[6] show that in some bias conditions many-body corrections might be needed to explain the observed noise suppression. Other experiments show that at low temperature suspended ropes of single-wall carbon nanotubes of length 0.4 μm exhibit a significant suppression of current fluctuations by a factor smaller than 1/100 compared to full shot noise.[5] However, this experimental result is not supported by a convincing interpretation, since possible explanations extend from ballistic transport in a small number of tubes within a rope, to diffusive transport in a substantial fraction of the CNTs.

In this work, we present an expression for the shot noise power spectral density of ballistic quasi-one-dimensional channels based on a statistical approach relying on quantities obtained from Monte Carlo (MC) simulations of randomly injected electrons from the reservoirs. The expression is derived within the second quantization formalism, and simulations are based on the self-consistent (SC) solution of the three-dimensional (3D) Poisson and Schrödinger equations, within the nonequilibrium Green's function (NEGF) formalism.[15]

Our proposed expression generalizes the Landauer-Büttiker's noise formula including the effects of Coulomb

 ©2010 The American Physical Society

interaction, which is significant for a large class of devices, and in particular for one-dimensional conductors.

II. THEORY

According to Milatz's theorem,[16] the power spectral density of the noise current in the zero frequency limit can be written as $S(0)=\lim_{1/\nu\to\infty}[2/\nu\cdot var(I)]$, where ν is the injection rate of a carrier from a contact and $var(I)$ is the variance of the current. According to Ref. 17, ν can be expressed as $\nu=\Delta E/(2\pi\hbar)$ where ΔE is the energy discretization step, i.e., the minimum energy separation between injected states. Indeed, the contribution to the current of a transverse mode in the energy interval ΔE can be expressed in the zero-temperature limit by the Landauer-Büttiker formula as $\langle dI\rangle = e/(2\pi\hbar)\Delta E$. On the other hand $\langle dI\rangle = e\nu$, from which $\nu = \Delta E/(2\pi\hbar)$ derives. Finally, the power spectral density of shot noise at zero frequency can be expressed as

$$S(0) = \lim_{\nu\to 0}\frac{2}{\nu}var(I) = \lim_{\Delta E\to 0} 4\pi\hbar\frac{var(I)}{\Delta E}. \tag{1}$$

The variance of the current can be derived by means of the second quantization formalism, which allows a concise treatment of the many-electron problem.

Let us consider a mesoscopic conductor connected to two reservoirs [source (S) and drain (D)], where electron states are populated according to their Fermi occupation factors (Fig. 1). For simplicity, we assume that the conductor is sufficiently short as to completely neglect inelastic scattering events. Thermalization occurs only in the reservoirs. At zero magnetic field and far from the interacting channel, the time-dependent current operator at the source can be expressed as the difference between the occupation number of carriers moving inward (N^{+}_{Sm}) and outward (N^{-}_{Sm}) in each quantum channel m,[13]

$$I(t) = \frac{e}{h}\sum_{m\in S}\int dE[N^{+}_{Sm}(E,t) - N^{-}_{Sm}(E,t)], \tag{2}$$

where

$$N^{+}_{Sm}(E,t) = \int d(\hbar\omega)a^{+}_{Sm}(E)a_{Sm}(E+\hbar\omega)e^{-i\omega t},$$

$$N^{-}_{Sm}(E,t) = \int d(\hbar\omega)b^{+}_{Sm}(E)b_{Sm}(E+\hbar\omega)e^{-i\omega t}. \tag{3}$$

The introduced operators $a^{\dagger}_{Sm}(E)$ and $a_{Sm}(E)$ create and annihilate, respectively, incident electrons in the source lead with total energy E in the channel m (Fig. 1). In the same way, the creation $b^{\dagger}_{Sm}(E)$ and annihilation $b_{Sm}(E)$ operators refer to electrons in the source contact for outgoing states. The channel index m runs over all the transverse modes and different spin orientations.

The operators a and b are related via a unitary transformation ($n=1,\ldots,W_S$),[13]

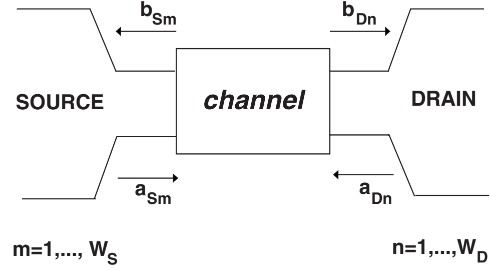

FIG. 1. Annihilation operators for ingoing (a_{Sm}, a_{Dn}) and outgoing electron states (b_{Sm}, b_{Dn}) in a two terminal scattering problem ($m=1,\ldots,W_S; n=1,\ldots,W_D$).

$$b_{Sn}(E) = \sum_{m=1}^{W_S}\mathbf{r}_{nm}(E)a_{Sm}(E) + \sum_{m=1}^{W_D}\mathbf{t}'_{nm}(E)a_{Dm}(E), \tag{4}$$

where W_S and W_D represent the number of quantum channels in the source and drain leads, respectively, while the blocks $\mathbf{r}$ (size $W_S\times W_S$) and $\mathbf{t}'$ (size $W_S\times W_D$), describe electron reflection at the source ($\mathbf{r}$) and transmission from drain to source ($\mathbf{t}'$) and are included in the scattering matrix $\mathbf{s}$ as[18]

$$\mathbf{s} = \begin{pmatrix} \mathbf{r} & \mathbf{t}' \\ \mathbf{t} & \mathbf{r}' \end{pmatrix}. \tag{5}$$

The dimensions of $\mathbf{s}$ are $(W_S+W_D)\times(W_S+W_D)$. Blocks $\mathbf{t}$ and $\mathbf{r}'$ in Eq. (5) are related to source-to-drain transmission and reflection back to the drain, respectively. In the following, time dependence will be neglected, since we are interested to the zero frequency case.

If we denote with $|\sigma\rangle$ a many-particle (antisymmetrical) state, the occupation number in the reservoir α in the channel m can be expressed as $\sigma_{\alpha m}(E) = \langle a^{\dagger}_{\alpha m}(E)a_{\alpha m}(E)\rangle_\sigma$. Pauli exclusion principle does not allow two electrons to occupy the same spin orbital, therefore $\sigma_{\alpha m}(E)$ can be either 0 or 1. In addition, since fluctuations of the potential profile along the channel due to Coulomb interaction between randomly injected carriers affect the transmission of electrons, the scattering matrix elements have to depend on the occupation numbers of all states in both reservoirs: $\mathbf{s}(E) = \mathbf{s}[\sigma_{S1}(E),\sigma_{S2}(E),\cdots,\sigma_{D1}(E),\sigma_{D2}(E),\cdots]$. Let us stress the fact that, as pointed out in Ref. 13, whenever a finite channel is connected to semi-infinite leads, the channel can be considered as a small perturbation to the equilibrium regime of the contacts, and independent random statistics can be used for both reservoirs.

According to Ref. 13, current fluctuations can be evaluated by introducing an ensemble of many electrons states $\{|\sigma_1\rangle,|\sigma_2\rangle,|\sigma_3\rangle,\cdots,|\sigma_N\rangle\}$ and by weighting each state properly, i.e., by finding its statistical average, denoted by $\langle\,\rangle_s$. Each reservoir $\alpha(\alpha=S,D)$ is assumed to be at thermal equilibrium, so that its average occupancy can be described by the Fermi-Dirac statistics f_α. As a consequence, the statistical average of $\sigma_{\alpha m}(E)$ reads,[13]

$$\langle\sigma_{\alpha m}(E)\rangle_s = \langle\langle a^{\dagger}_{\alpha m}(E)a_{\alpha m}(E)\rangle_\sigma\rangle_s = f_\alpha(E). \tag{6}$$

Neglecting correlations between the occupation numbers of the same quantum channel at different energies, or between

different channels at the same energy, we obtain,[13]

$$\langle \sigma_{\alpha m}(E)\sigma_{\beta n}(E')\rangle_s = f_\alpha(E) f_\beta(E'), \tag{7}$$

for $\alpha \neq \beta$ or $m \neq n$ or $E \neq E'$. Including Eq. (6) in Eq. (7) and exploiting the relation $\sigma_{\alpha m}(E)^2 = \sigma_{\alpha m}(E)$, the average of the product of two occupation numbers can be expressed as

$$\langle \sigma_{\alpha m}(E)\sigma_{\beta n}(E')\rangle_s = f_\alpha(E) f_\beta(E') + \delta(E-E')\,\delta_{\alpha\beta}\delta_{mn}[f_\alpha(E) - f_\alpha(E) f_\beta(E')], \tag{8}$$

where $\delta(E-E')$, $\delta_{\alpha\beta}$, δ_{mn} are Kronecker delta functions.

In order to compute the average current along the channel and the power spectral density of the current fluctuations, we need to write the expectation values of the products of two and four operators,[13]

$$\langle a^\dagger_{\alpha m}(E) a_{\beta n}(E')\rangle_\sigma = \delta(E-E')\,\delta_{\alpha\beta}\delta_{mn}\sigma_{\alpha m}(E), \tag{9}$$

$$\begin{aligned}\langle a^\dagger_{\alpha m}(E) a_{\beta n}(E') a^\dagger_{\gamma k}(E'') a_{\delta l}(E''')\rangle_\sigma &= \delta(E-E''')\,\delta(E'-E'')\,\delta_{\alpha\delta}\delta_{ml}\delta_{\beta\gamma}\delta_{nk}\sigma_{\alpha m}(E)[1-\sigma_{\gamma k}(E'')] \\ &\quad + \delta(E-E')\,\delta(E''-E''')\,\delta_{\alpha\beta}\delta_{nm}\delta_{\gamma\delta}\delta_{kl}\sigma_{\alpha m}(E)\sigma_{\gamma k}(E''),\end{aligned} \tag{10}$$

where the first contribution in Eq. (10) refers to exchange pairing ($\alpha=\delta$, $\beta=\gamma$, $m=l$, $n=k$), while the second to normal pairing ($\alpha=\beta$, $\gamma=\delta$, $m=n$, $k=l$).[13] For the sake of simplicity, in the following we denote the expectation $\langle\langle\ \rangle_\sigma\rangle_s$ as $\langle\ \rangle$.

By means of Eqs. (4) and (9) the average current reads

$$\begin{aligned}\langle I\rangle &= \frac{e}{h}\int dE\left\{\sum_{n\in S}\langle[\mathbf{t}^\dagger\mathbf{t}]_{nn}\sigma_{Sn}\rangle_s - \sum_{k\in D}\langle[\mathbf{t}'^\dagger\mathbf{t}']_{kk}\sigma_{Dk}\rangle_s\right\} \\ &= \frac{e}{h}\int dE\left\{\sum_{n\in S}\langle[\tilde{\mathbf{t}}]_{S;nn}\sigma_{Sn}\rangle_s - \sum_{k\in D}\langle[\tilde{\mathbf{t}}]_{D;kk}\sigma_{Dk}\rangle_s\right\},\end{aligned} \tag{11}$$

where $[\tilde{\mathbf{t}}]_{\alpha;lp} \equiv [\mathbf{t}^\dagger\mathbf{t}]_{lp}$ if $\alpha=S$ and $[\mathbf{t}'^\dagger\mathbf{t}']_{lp}$ if $\alpha=D$ $(l,p\in\alpha)$. The unitarity of the matrix $\mathbf{s}$ has also been exploited, from which the relation $\mathbf{r}^\dagger\mathbf{r}+\mathbf{t}^\dagger\mathbf{t}=\mathbf{1}$ follows. It is easy to show that for a non-interacting channel, i.e., when occupancy of injected states does not affect transmission and reflection probabilities, Eq. (11) reduces to the two-terminal Landauer's formula.[19]

In general, we can observe that for an interacting channel Eq. (11) provides a different result with respect to Landauer's formula, because fluctuation of transmission probabilities induced by random injection in the device, is responsible for rectification of the current. The effect is often very small, but not always.[20] However, it cannot be captured by Landauer's formula, as other many-particle processes affecting device transport properties.[21,22]

The mean squared current reads

$$\begin{aligned}\langle I^2\rangle = \left(\frac{e}{h}\right)^2\int dE\int dE' \sum_{m,n\in S}\{&\langle N^+_{Sm}(E)N^+_{Sn}(E')\rangle \\ &- \langle N^+_{Sm}(E)N^-_{Sn}(E')\rangle - \langle N^-_{Sm}(E)N^+_{Sn}(E')\rangle \\ &+ \langle N^-_{Sm}(E)N^-_{Sn}(E')\rangle\} = F_{++}+F_{+-}+F_{-+}+F_{--}.\end{aligned} \tag{12}$$

This expression consists of four terms, related to states at the source contacts, that can be evaluated by means of Eqs. (9) and (10), the first one (F_{++}) represents the correlation of fluctuations in two ingoing streams, the second and the third ones (F_{+-}, F_{-+}) describe the correlations of the fluctuations of the ingoing and outgoing streams, the fourth one (F_{--}) refers to two outgoing streams.

The first term F_{++} can be expressed as

$$F_{++} = \left(\frac{e}{h}\right)^2\int dE\int dE' \sum_{m,n\in S}\langle\sigma_{Sm}(E)\sigma_{Sn}(E')\rangle_s, \tag{13}$$

since $\langle\sigma^2_{Sm}(E)\rangle_s = \langle\sigma_{Sm}(E)\rangle_s = f_S(E)$ $\forall m\in S$. Correlations between ingoing states are established through the statistical expectation values of each couple of occupancies of states injected from the source.

The second contribution F_{+-} reads

$$\begin{aligned}F_{+-} = -\left(\frac{e}{h}\right)^2\int dE\int dE'\Bigg\{&\sum_{m,l\in S}\langle(1 - [\tilde{\mathbf{t}}(E')]_{S;ll})\sigma_{Sm}(E)\sigma_{Sl}(E')\rangle_s \\ &+ \sum_{m\in S}\sum_{k\in D}\langle[\tilde{\mathbf{t}}(E')]_{D;kk}\sigma_{Sm}(E)\sigma_{Dk}(E')\rangle_s\Bigg\},\end{aligned} \tag{14}$$

since $\sigma^2_{\alpha l}(E) = \sigma_{\alpha l}(E)$ $\forall l\in\alpha$ $(\alpha=S,D)$, due to the Pauli exclusion principle. In Eq. (14) correlations between ingoing and outgoing states are obtained by summing on each statistical average of the product of two occupation numbers of injected states, weighted with the reflection $(1-[\tilde{\mathbf{t}}(E')]_{S;ll} = [\mathbf{r}^\dagger\mathbf{r}(E')]_{ll})$ or transmission probability ($[\tilde{\mathbf{t}}(E')]_{D;kk}$) of outgoing channels.

By exploiting the anticommutation relations of the fermionic operators a, it is simple to demonstrate that the third term F_{-+} is identical to F_{+-}. Indeed,

$$\langle N^-_{Sm}(E)N^+_{Sn}(E')\rangle = \langle N^+_{Sn}(E')N^-_{Sm}(E)\rangle. \tag{15}$$

Finally, the fourth term F_{--} reads:

$$\begin{aligned}F_{--} &= \left(\frac{e}{h}\right)^2\Delta E\int dE\sum_{\alpha=S,D}\sum_{l\in\alpha}\langle[\tilde{\mathbf{t}}]_{\alpha;ll}(1-[\tilde{\mathbf{t}}]_{\alpha;ll})\sigma_{\alpha l}\rangle_s \\ &\quad - \left(\frac{e}{h}\right)^2\Delta E\int dE\sum_{\alpha=S,D}\sum_{\substack{l,p\in\alpha\\ l\neq p}}\langle[\tilde{\mathbf{t}}]_{\alpha;lp}[\tilde{\mathbf{t}}]_{\alpha;pl}\sigma_{\alpha l}\sigma_{\alpha p}\rangle_s \\ &\quad - 2\left(\frac{e}{h}\right)^2\Delta E\int dE\sum_{k\in D}\sum_{p\in S}\langle[\mathbf{t}'^\dagger\mathbf{r}]_{kp}[\mathbf{r}^\dagger\mathbf{t}']_{pk}\sigma_{Dk}\sigma_{Sp}\rangle_s \\ &\quad + \left\langle\left[\frac{e}{h}\int dE\left(\sum_{l\in S}[\tilde{\mathbf{t}}]_{S;ll}\sigma_{Sl} - \sum_{k\in D}[\tilde{\mathbf{t}}]_{D;kk}\sigma_{Dk}\right)\right]^2\right\rangle_s\end{aligned}$$

$$+2\left(\frac{e}{h}\right)^2\int dE\int dE'\sum_{l\in S}\sum_{k\in D}$$
$$\times\langle[\tilde{\mathbf{t}}(E')]_{D;kk}\sigma_{Sl}(E)\sigma_{Dk}(E')\rangle_s$$
$$-2\left(\frac{e}{h}\right)^2\int dE\int dE'\sum_{l,p\in S}\langle[\tilde{\mathbf{t}}(E)]_{S;ll}\sigma_{Sl}(E)\sigma_{Sp}(E')\rangle_s$$
$$+\left(\frac{e}{h}\right)^2\int dE\int dE'\sum_{l,p\in S}\langle\sigma_{Sl}(E)\sigma_{Sp}(E')\rangle_s. \quad (16)$$

Equation (16) contains all correlations between outgoing electron states in the source lead, where outgoing carriers at the source can be either reflected carriers incident from S or transmitted carriers injected from D. By means of the Eqs. (13), (14), and (16), we find the mean squared current

$$\langle I^2\rangle=\left(\frac{e}{h}\right)^2\Delta E\int dE\sum_{\alpha=S,D}\sum_{l\in\alpha}\langle[\tilde{\mathbf{t}}]_{\alpha;ll}(1-[\tilde{\mathbf{t}}]_{\alpha;ll})\sigma_{\alpha l}\rangle_s$$
$$-\left(\frac{e}{h}\right)^2\Delta E\int dE\sum_{\alpha=S,D}\sum_{\substack{l,p\in\alpha\\ l\neq p}}\langle[\tilde{\mathbf{t}}]_{\alpha;lp}[\tilde{\mathbf{t}}]_{\alpha;pl}\sigma_{\alpha l}\sigma_{\alpha p}\rangle_s$$
$$-2\left(\frac{e}{h}\right)^2\Delta E\int dE\sum_{k\in D}\sum_{p\in S}\langle[\mathbf{t}'^{\dagger}\mathbf{r}]_{kp}[\mathbf{r}^{\dagger}\mathbf{t}']_{pk}\sigma_{Dk}\sigma_{Sp}\rangle_s$$
$$+\left\langle\left[\frac{e}{h}\int dE\left(\sum_{l\in S}[\tilde{\mathbf{t}}]_{S;ll}\sigma_{Sl}-\sum_{k\in D}[\tilde{\mathbf{t}}]_{D;kk}\sigma_{Dk}\right)\right]^2\right\rangle_s. \quad (17)$$

Finally, from Eqs. (1), (11), and (17) the noise power spectrum can be expressed as

$$S(0)=\left(\frac{e^2}{\pi\hbar}\right)\int dE\sum_{\alpha=S,D}\sum_{l\in\alpha}\langle[\tilde{\mathbf{t}}]_{\alpha;ll}(1-[\tilde{\mathbf{t}}]_{\alpha;ll})\sigma_{\alpha l}\rangle_s$$
$$-\left(\frac{e^2}{\pi\hbar}\right)\int dE\sum_{\alpha=S,D}\sum_{\substack{l,p\in\alpha\\ l\neq p}}\langle[\tilde{\mathbf{t}}]_{\alpha;lp}[\tilde{\mathbf{t}}]_{\alpha;pl}\sigma_{\alpha l}\sigma_{\alpha p}\rangle_s$$
$$-2\left(\frac{e^2}{\pi\hbar}\right)\int dE\sum_{k\in D}\sum_{p\in S}\langle[\mathbf{t}'^{\dagger}\mathbf{r}]_{kp}[\mathbf{r}^{\dagger}\mathbf{t}']_{pk}\sigma_{Dk}\sigma_{Sp}\rangle_s$$
$$+\frac{4\pi\hbar}{\Delta E}var\left\{\frac{e}{h}\int dE\left(\sum_{n\in S}[\tilde{\mathbf{t}}]_{S;nn}\sigma_{Sn}-\sum_{k\in D}[\tilde{\mathbf{t}}]_{D;kk}\sigma_{Dk}\right)\right\}. \quad (18)$$

Equation (18) is the main theoretical result of this work, the power spectral density of the noise current is expressed in terms of transmission $(\mathbf{t},\mathbf{t}')$, reflection $(\mathbf{r})$ amplitude matrices, and properties of the leads, such as random occupation numbers of injected states. Let us point out that, although our derivation starts from Eq. (2), which is valid only far from the mesoscopic interacting sample, Eq. (18) allows to take into account both Pauli and Coulomb interactions through the dependence of $\mathbf{t}$, $\mathbf{t}'$ and $\mathbf{r}$ on actually injected states. Let us note that we go beyond the Hartree approximation by considering different random configuration of injected electron states for different many-particle systems.

There is a crucial difference with respect to Landauer-Büttiker's formula, since Eq. (18) enables to consider fluctuations in time of the potential profile along the channel induced by the electrostatic repulsion between randomly injected electrons from the leads. Essentially, for each random configuration of injected states from both reservoirs, we consider a *snapshot* of device operation at a different time instant. All statistical properties—in the limit of zero frequency—can be obtained by considering a sufficient ensemble of snapshots.

Let us discuss some physical limits of interest. First, we consider the case of zero temperature. In such condition the Fermi factor for populating electron states in the reservoirs is either 0 or 1, and all snapshots are identical, so the fourth term in Eq. (18) disappears. In addition, we can remove the statistical averaging in Eq. (18) and the first three terms lead to the following expression of the noise power spectrum,

$$S(0)=\frac{2e^2}{\pi\hbar}\int_{E_{FD}}^{E_{FS}}dE(\mathrm{Tr}[\mathbf{t}^{\dagger}\mathbf{t}]-\mathrm{Tr}[\mathbf{t}^{\dagger}\mathbf{t}\mathbf{t}^{\dagger}\mathbf{t}]), \quad (19)$$

where E_{FS} and E_{FD} are the Fermi energies of the source and drain contacts, respectively. Such terms can be identified with partition noise (PN) contribution. More in detail, the first term of Eq. (18) is associated to the quantum uncertainty of whether an electron injected in the mode l from the reservoir α is transmitted through or reflected by the barrier.

The second term of Eq. (18) contains instead $(l\neq p)$,

$$[\mathbf{t}^{\dagger}\mathbf{t}]_{lp}[\mathbf{t}^{\dagger}\mathbf{t}]_{pl}=\sum_{k,q\in D}\mathbf{t}^*_{kl}\mathbf{t}_{kp}\mathbf{t}^*_{qp}\mathbf{t}_{ql}. \quad (20)$$

Each term of the sum can be interpreted as the coupling between a transmission event from channel $p\in S$ into channel $k\in D$ and from channel $l\in S$ into channel $q\in D$, such a coupling is due to time-reversed transmissions from k into l and from q into p.

In the same way, the third term of Eq. (18) contains

$$[\mathbf{t}'^{\dagger}\mathbf{r}]_{kp}[\mathbf{r}^{\dagger}\mathbf{t}']_{pk}=\sum_{l,n\in S}\mathbf{t}^*_{kl}\mathbf{r}_{lp}\mathbf{r}^*_{np}\mathbf{t}_{kn}, \quad (21)$$

which represents the coupling between carriers transmitted from $n\in S$ into $k\in D$ and reflected from $p\in S$ into $l\in S$. The second and third terms provide insights on exchange effects. Indeed, in such terms, contributions with $k\neq q$ and $l\neq n$, respectively, are complex and they represent exchange interference effects (fourth-order interference effects) in the many-particle wave function due to the quantum-mechanical impossibility to distinguish identical carriers.[17] In the Sec. IV, we will be concerned with identical reservoirs, i.e., identical injected modes from the contacts. In this case the diagonal terms of the partition noise [first term and part of the third term in Eq. (18)] will be referred as on-diagonal partition noise (PN ON), while the off-diagonal ones [second term and part of the third term in Eq. (18)] will be denoted as off-diagonal contribution to the partition noise (PN OFF).

Now let us assume that the number of quantum channel in the source is smaller than the one in the drain $(W_S\leq W_D)$ and let us consider the case of potential barrier wide with respect

to the wavelength, so that one may neglect tunneling. In such a situation, the reflection amplitude matrix $\mathbf{r}$ is equal to zero for energies larger than the barrier maximum E_C, whereas the transmission amplitude matrix is zero for energies smaller than E_C. By means of the unitarity of the scattering matrix $\mathbf{s}$, follows $\mathbf{t}^\dagger\mathbf{t}=\mathbf{I}_S$ for $E>E_C$, where $\mathbf{I}_S$ is the identity matrix of order W_S. Due to reversal time symmetry, there are W_S completely opened quantum channels in the drain contact and W_D-W_S completely closed. In this situation only the fourth term in Eq. (18) survives and the noise power spectral density becomes

$$S(0)=\frac{2e^2W_S}{\pi\hbar}\int_{E_C}^{+\infty}dE[f_S(1-f_S)+f_D(1-f_D)] =\frac{2e^2kTW_S}{\pi\hbar}[f_S(E_C)+f_D(E_C)]. \tag{22}$$

When $E_{FS}=E_{FD}$ such term obviously reduces to the thermal noise spectrum $4kTG$, where $G=[e^2W_Sf_S(E_C)]/(\pi\hbar)$ is the channel conductance at equilibrium. The fourth term in Eq. (18) can be therefore identified with the injection noise (IN) contribution.

Equation (18) describes correlations between transmitted states coming from the same reservoirs [second term in Eq. (18)] and between transmitted and reflected states in the source lead (third term), with a contribution of opposite sign with respect to the first term. The negative sign derives from Eq. (10), in which exchange pairings include a minus sign due to the fermionic nature of electrons. Note that Eq. (18) can be expressed in a symmetric form with respect to an exchange between the source and the drain contacts. Indeed, by exploiting the unitarity of the scattering matrix, the third term becomes,

$$-\left(\frac{e^2}{\pi\hbar}\right)\int dE\sum_{k\in D}\sum_{p\in S}\langle[\mathbf{t}'^\dagger\mathbf{r}]_{kp}[\mathbf{r}^\dagger\mathbf{t}']_{pk}\sigma_{Dk}\sigma_{Sp}\rangle_s -\left(\frac{e^2}{\pi\hbar}\right)\int dE\sum_{k\in D}\sum_{p\in S}\langle[\mathbf{r}'^\dagger\mathbf{t}]_{kp}[\mathbf{t}^\dagger\mathbf{r}']_{pk}\sigma_{Dk}\sigma_{Sp}\rangle_s, \tag{23}$$

which establishes correlations between transmitted and reflected states in the source and drain leads.

Now let us consider the limit when transmission and reflection matrices do not depend on random occupation numbers of injected states, i.e., a nonfluctuating potential profile is imposed along the channel. By exploiting the reversal time symmetry ($\mathbf{s}=\mathbf{s}^{\mathbf{t}}$, so that $\mathbf{t}'=\mathbf{t}^{\mathbf{t}}$), the unitarity of the scattering matrix, Eq. (18) reduces to Landauer-Büttiker's noise formula,[13]

$$S(0)=\frac{2e^2}{\pi\hbar}\Bigg\{\int dE\sum_{\alpha=S,D}(\mathrm{Tr}[\mathbf{t}^\dagger\mathbf{t}]-\mathrm{Tr}[\mathbf{t}^\dagger\mathbf{t}\mathbf{t}^\dagger\mathbf{t}]+T_\alpha)f_\alpha -\int dE\sum_{\alpha=S,D}T_\alpha f_\alpha^2-2\int dE(\mathrm{Tr}[\mathbf{t}^\dagger\mathbf{t}]-\mathrm{Tr}[\mathbf{t}^\dagger\mathbf{t}\mathbf{t}^\dagger\mathbf{t}])f_Sf_D +\int dE\sum_{\alpha=S,D}(\mathrm{Tr}[\mathbf{t}^\dagger\mathbf{t}\mathbf{t}^\dagger\mathbf{t}]-T_\alpha)[f_\alpha(1-f_\alpha)]\Bigg\}, \tag{24}$$

where $T_\alpha=\Sigma_{l\neq p\in\alpha}[\tilde{\mathbf{t}}]_{\alpha;lp}[\tilde{\mathbf{t}}]_{\alpha;pl}$ and the sum does not run on the spin. Equation (24) then reduces to

$$S(0)=\frac{2e^2}{\pi\hbar}\int dE\{[f_S(1-f_S)+f_D(1-f_D)]\mathrm{Tr}[\mathbf{t}^\dagger\mathbf{t}\mathbf{t}^\dagger\mathbf{t}] +[f_S(1-f_D)+f_D(1-f_S)](\mathrm{Tr}[\mathbf{t}^\dagger\mathbf{t}]-\mathrm{Tr}[\mathbf{t}^\dagger\mathbf{t}\mathbf{t}^\dagger\mathbf{t}])\}. \tag{25}$$

Let us note that Eq. (19) can be recovered as well from Eq. (25). Indeed at zero temperature the stochastic injection vanishes since random statistics coincides to the Fermi factor. In the same way, Eq. (22) might be derived from Eq. (25), since in this case noise is only due to the thermionic emission contribution and fluctuations of the potential profile do not play any role in noise.

III. COMPUTATIONAL METHODOLOGY AND QUANTITATIVE ANALYSIS

In order to properly include the effect of Coulomb interaction, we self-consistently solve the 3D Poisson equation, coupled with the Schrödinger equation with open boundary conditions, within the NEGF formalism, which has been implemented in our in-house open source simulator NANOTCAD VIDES.[23] For what concerns the boundary conditions of Poisson equations, Dirichlet boundary conditions are imposed in correspondence of the metal gates, whereas null Neumann boundary conditions are applied on the ungated surfaces of the 3D simulation domain. In particular the 3D Poisson equation reads

$$\vec{\nabla}\cdot[\epsilon\vec{\nabla}\phi(\vec{r})]=-[\rho(\vec{r})+\rho_{fix}(\vec{r})], \tag{26}$$

where ϕ is the electrostatic potential, ρ_{fix} is the fixed charge, which accounts for ionized impurities in the doped regions, and ρ is the charge density per unit volume,

$$\rho(\vec{r})=-e\int_{E_i}^{+\infty}dE\sum_{\alpha=S,D}\sum_{n\in\alpha}DOS_{\alpha n}(\vec{r},E)\sigma_{\alpha n}(E) +e\int_{-\infty}^{E_i}dE\sum_{\alpha=S,D}\sum_{n\in\alpha}DOS_{\alpha n}(\vec{r},E)[1-\sigma_{\alpha n}(E)], \tag{27}$$

where E_i is the midgap potential, $DOS_{\alpha n}(\vec{r},E)$ is the local density of states associated to channel n injected from contact α and $\vec{r}$ is the 3D spatial coordinate.

From a computational point of view, modeling of the stochastic injection of electrons from the reservoirs has been performed by means of statistical simulations taking into account an ensemble of many electron states, i.e., an ensemble of random configurations of injected electron states, from both contacts. In particular, the whole energy range of integration [Eqs. (18) and (27)] has been uniformly discretized with energy step ΔE. Then, in order to obtain a random injection configuration, a random number r uniformly distributed between 0 and 1 has been extracted for each electron state represented by energy E, reservoir α and quantum channel n.[24] More in detail, the state is occupied if r is

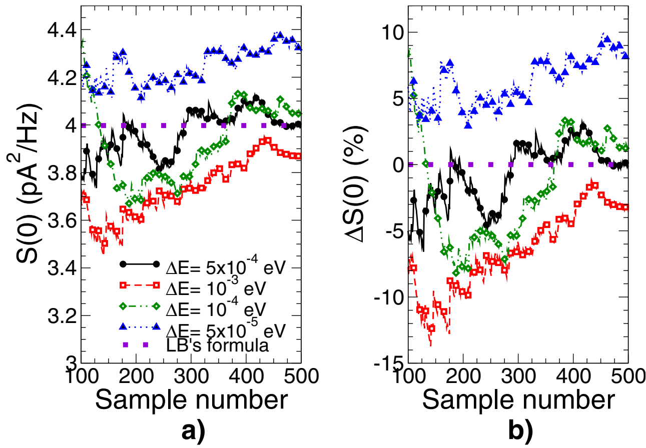

FIG. 2. (Color online) a) Noise power spectral density $S(0)$ obtained from Eq. (18) for a given potential as a function of current sample number for four different energy steps. b) Relative deviation of $S(0)$ with respect to Landauer-Büttiker's limit Eq. (25). The simulated structure is the SNW-FET shown in Fig. 3.

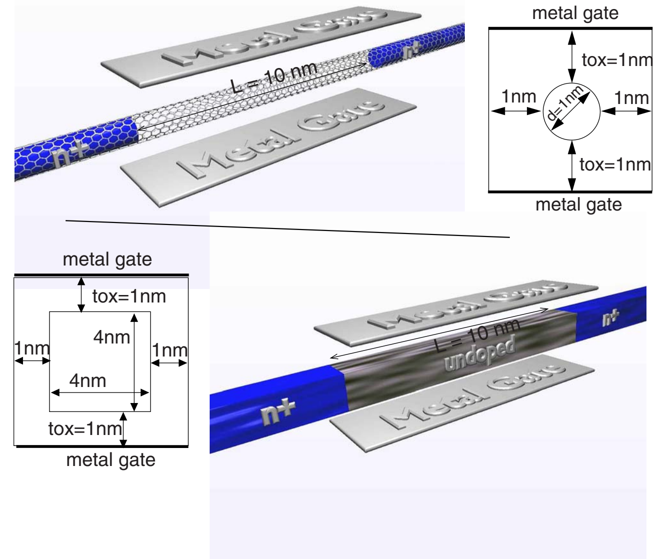

FIG. 3. (Color online) 3D structures and transversal cross sections of the simulated CNT (top) and SNW-FETs (bottom).

smaller than the Fermi-Dirac factor, i.e., $\sigma_{Sn}(E)[\sigma_{Dn}(E)]$ is 1 if $r < f_S(E)[f_D(E)]$, and 0 otherwise.

The random injection configuration generated in this way has been then inserted in Eq. (27) and self-consistent solution of Eqs. (26) and (27) and the Schrödinger equations has been performed. Once convergence has been reached, the transmission $(\mathbf{t},\mathbf{t}')$ and reflection $(\mathbf{r})$ matrices are computed. The procedure is repeated several times in order to gather data from a reasonable ensemble. In our case, we have verified that an ensemble of 500 random configurations represents a good trade-off between computational cost and accuracy. Finally, the power spectral density $S(0)$ has been extracted by means of Eq. (18).

In the following, we will refer to self-consistent Monte Carlo simulations (SC-MC), when statistical simulations using the procedure described above, i.e., inserting random occupations $\sigma_{Sn}(E)$ and $\sigma_{Dn}(E)$ in Eq. (27), are performed. Instead, we will refer to SC simulations when the Poisson-Schrödinger equations are solved considering f_S and f_D in Eq. (27). SC-MC simulations of randomly injected electrons allow considering both the effect of Pauli and Coulomb interaction on noise.

From a numerical point of view, particular attention has to be posed on the choice of the energy step ΔE. In Fig. 2 the noise power spectrum computed by keeping fixed the potential profile along the channel and performing statistical Monte Carlo simulations of randomly injected electrons is shown for four energy steps. As already proved in Eq. (24), the convergence to Landauer-Büttiker's limit is ensured for all the considered energy steps: as can be seen, $\Delta E = 5 \times 10^{-4}$ eV provides faster convergence as compared to the other values with a relative error close to 0.16%.

Let us point out that the NEGF formalism computes directly the total Green's function $\mathbf{G}$ of the channel and the broadening function of the source $(\mathbf{\Gamma}_S)$ and drain $(\mathbf{\Gamma}_D)$ leads, rather than the scattering matrix $\mathbf{s}$, that relates the outgoing waves amplitudes to the incoming waves amplitudes at different reservoirs. In order to obtain the matrix $\mathbf{s}$, we have exploited the *Fisher-Lee relation*,[25] which expresses the elements of the $\mathbf{s}$-matrix in terms of the Green's function $\mathbf{G}$ and transverse mode eigenfunctions (see Appendix).

IV. RESULTS

The approach described in the previous section has been used to study the behavior of shot noise in quasi-one-dimensional (1D) channel of CNT-FETs and SNW-FETs with identical reservoirs (Fig. 3). We consider a (13,0) CNT embedded in SiO_2 with oxide thickness equal to 1 nm, an undoped channel of 10 nm and n-doped CNT extensions 10 nm long, with a molar fraction $f = 5 \times 10^{-3}$. The SNW-FET has an oxide thickness (t_{ox}) equal to 1 nm and the channel length (L) is 10 nm. The channel is undoped and the source and drain extensions (10 nm long) are doped with $N_D = 10^{20}$ cm^{-3}. The device cross section is 4×4 nm^2.

From a numerical point of view, a p_z-orbital tight-binding Hamiltonian has been assumed for CNTs,[26,27] whereas an effective mass approximation has been considered for SNWs[28,29] by means of an adiabatic decoupling in a set of two-dimensional equations in the transversal plane and in a set of one-dimensional equations in the longitudinal direction for each 1D subband. For both devices, we have developed a quantum ballistic transport model with semi-infinite extensions at their ends. A mode space approach has been adopted, since only the lowest sub-bands take part to transport. In particular, we have verified that four modes are enough to compute the mean current both in the ohmic and saturation regions. All calculations have been performed at room temperature $(T = 300$ K$)$.

Let us focus our attention on the Fano factor F, defined as the ratio of the actual noise power spectrum $S(0)$ to the full shot noise $2q\langle I \rangle$. In Figs. 4 and 5 the contributions to F of

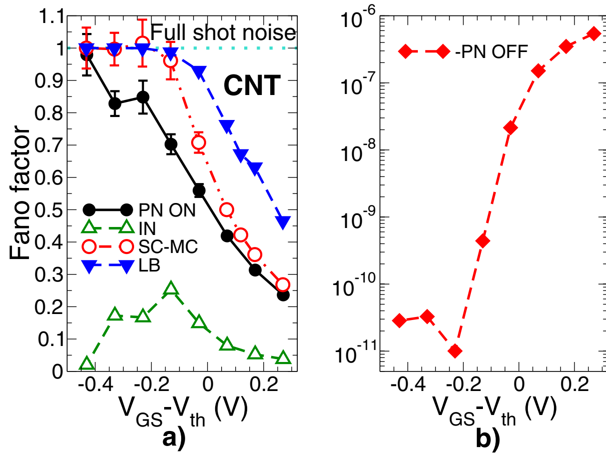

FIG. 4. (Color online) Contributions to the Fano factor in a CNT-FET of the on-diagonal and off-diagonal partition noise and of the injection noise [respectively, on-diagonal and off-diagonal part of the first three terms, and fourth term in Eq. (18)] as a function of the gate overdrive $V_{GS}-V_{th}$ for a drain-to-source bias V_{DS}=0.5 V. a) The on-diagonal partition (PN ON, solid circles), the injection (IN, open triangles up) and the full noise (open circles) computed by means of SC-MC simulations are shown. The Fano factor computed by exploiting Landauer-Büttiker's formula (25) and SC simulations (solid triangles down) is also shown. b) Off-diagonal partition noise contribution (PN OFF) to F due to correlation between transmitted states and between transmitted and reflected states.

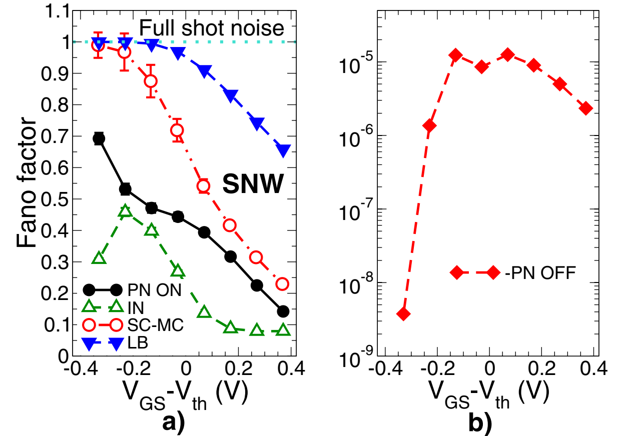

FIG. 5. (Color online) Contributions to the Fano factor in a SNW-FET of the on-diagonal and off-diagonal partition noise and of the injection noise, obtained for V_{DS}=0.5 V, as a function of the gate overdrive $V_{GS}-V_{th}$ in a SNW-FET. In a) the on-diagonal partition, the injection and the full noise computed by means of SC-MC simulations (both Pauli and Coulomb interactions taken into account) are shown together with results obtained by means of Eq. (25). b) Off-diagonal partition noise due to correlation between transmitted states and between transmitted and reflected states.

partition noise [first three terms in Eq. (18)] and injection noise (fourth term in Eq. (18)) are shown, as a function of the gate overdrive $V_{GS}-V_{th}$ for a drain-to-source bias V_{DS} =0.5 V for CNT-FETs and SNW-FETs, respectively, results have been obtained by means of SC-MC simulations. The threshold voltage V_{th} at V_{DS}=0.5 V is 0.43 V for the CNT-FET and 0.13 V for the SNW-FET. In particular, Figs. 4(a) and 5(a) refer to the on-diagonal contribution to the partition noise (solid circles), to the injection noise (open triangles up) and to the complete Fano factor (open circles) obtained by means of Eq. (18), i.e., Pauli and Coulomb interactions simultaneously considered. We present also the Fano factor (solid triangles down) computed by applying Eq. (25) on the self-consistent potential profile, i.e., when only Pauli exclusion principle is included. In Figs. 4(b) and 5(b) we show the contribution of the off-diagonal partition noise to F, which provides a measure of mode-mixing and of exchange interference effects.

As can be seen in Figs. 4(a) and 5(a), in the subthreshold regime ($V_{GS}-V_{th}<-0.2$ V, $\langle I\rangle<10^{-9}$ A) the Poissonian noise for a nondegenerate injection is recovered, since electron-electron interactions are negligible due to the very small amount of mobile charge in the channel. In the strong inversion regime instead ($V_{GS}-V_{th}>0$ V, $\langle I\rangle>10^{-6}$ A), noise is greatly suppressed with respect to the full shot value. In particular for a SNW-FET, at $V_{GS}-V_{th}\approx 0.4$ V ($\langle I\rangle\approx 2.4\times 10^{-5}$ A), combined Pauli and Coulomb interactions suppress shot noise down to 22% of the full shot noise value, while for CNT-FET the Fano factor is equal to 0.27 at $V_{GS}-V_{th}\approx 0.3$ V ($\langle I\rangle\approx 1.4\times 10^{-5}$ A). This is due to the fact that as soon as an electron is injected, the barrier height along the channel increases, leading to a reduced transmission probability for other electrons.

As shown in Fig. 4(a), the dominant noise source in ballistic CNT-FETs is the on-diagonal partition noise and the noise due to the intrinsic thermal agitations of charge carriers in the contacts (injection noise), which is at most the 36% of the partition noise ($V_{GS}-V_{th}\approx -0.1$ V). Nearly identical results are shown for SNW-FETs, with the exception of a stronger contribution given by the injection noise, up to the 86% of the on-diagonal partition term ($V_{GS}-V_{th}\approx -0.2$ V). Moreover, the behavior of the two noise components, as a function of $V_{GS}-V_{th}$, is very similar for both CNT- and SNW-FETs, F tends to 1 in the subthreshold regime, while in strong inversion regime shot noise is strongly suppressed.

Let us stress that an SC-MC simulation exploiting Eq. (18) is mandatory for a quantitative evaluation of noise. Indeed, by only considering Pauli exclusion principle through formula (25), one would have overestimated shot noise by 180% for SNW-FET ($V_{GS}-V_{th}\approx 0.4$ V) and by 70% for CNT-FET ($V_{GS}-V_{th}\approx 0.3$ V).[20,24]

It is interesting to observe that the off-diagonal contribution to partition noise, due to exchange correlations between transmitted states and between transmitted and reflected states, has a strong dependence on the height of the potential profile along the channel (variation of 5 orders of magnitude for CNT-FETs) and is negligible for quasi one-dimensional FETs. In particular, for CNT-FETs such term is at most 5 orders of magnitude smaller than the on-diagonal partition noise or injection noise in the strong inversion regime ($V_{GS}-V_{th}\approx 0.3$ V), while in the subthreshold regime its magnitude still reduces (about 10^{-11} for $V_{GS}-V_{th}\approx -0.4$ V). For SNW-FETs we have obtained similar results, the off-diagonal partition noise is indeed at most 5 orders of magnitude smaller than the other two contributions.

In such conditions, transmission occurs only along separate quantum channels and an uncoupled mode approach is

also accurate. Indeed, off-diagonal partition noise provides interesting information on the strength of the mode-coupling, which, as already seen, is very small. In particular, neglecting this term, results obtained from Eq. (18) can be recovered as well.

In the previous discussion, carriers from different quantum channels do not interfere. However, since we deal with a many indistinguishable particle system, such effects can come into play. To this purpose, we investigate in more detail two examples, in which exchange pairings, that include also exchange interference effects, give a non-negligible contribution to drain current noise. In the past exchange interference effects have been already predicted for example in ballistic conductor with an elastic scattering center in the channel,[30] in diffusive four-terminal conductors of arbitrary shape[31] and in quantum dot in the quantum Hall regime,[32] connected to two leads via quantum point contacts.

In the first case, we discuss, mode-mixing does not appear, i.e., the nondiagonal elements of the matrices $\mathbf{t}^{\dagger}\mathbf{t}$ and $\mathbf{t}'^{\dagger}\mathbf{r}$ are negligible with respect to the diagonal ones. Since the off-diagonal partition noise is negligible and since in the third term in Eq. (18) only contributions with indices $l=n=k=p$ survive, exchange interference effects do not contribute to electrical noise. We consider a CNT-FET at low bias condition: $V_{DS}=50$ mV. In Fig. 6(a) the on-diagonal partition noise, the injection noise and correlations due to the off-diagonal partition noise, evaluated performing statistical SC-MC simulations, are shown. In this case, on-diagonal correlations between transmitted and reflected states in the source lead (in the same quantum channel) extremely affect noise. Indeed, at the energies at which reflection events in the source lead are allowed, also electrons coming from D can be transmitted into the injecting contact S, since the corresponding energy states in D are occupied and the barrier height is small. Instead the exchange correlations represented by the off-diagonal partition noise are negligible, since they are at least 5 order of magnitude smaller than the other three terms in Eq. (18). Note that the noise enhancement obtained both in the inversion and subthreshold regimes is due to the fact that at low bias the current $\langle I \rangle$ becomes small, while the noise power spectrum $S(0)$ tends to a finite value, because of the thermal noise contribution.

Let now consider the situation in which modes are coupled and exchange interference effects, through the off-diagonal partition noise, contribute to drain current fluctuations. We consider the interesting case in which a vacancy, i.e., a missing carbon atom, is placed at the center of the channel of a (13,0) CNT-FET. From a numerical point of view, this defect can be modeled by introducing a strong repulsive potential (i.e., +8 eV, much larger than the energy gap of a (13,0) CNT: $E_{gap}\approx 0.75$ eV) in correspondence of such site, thus acting as a barrier for transmission in the middle of the channel [Fig. 6(c)].

In Fig. 6(b) the three noise sources in Eq. (18) (on and off-diagonal partition noise, injection noise) are plotted as a function of the gate voltage V_{GS} in the above threshold regime for $V_{DS}=0.5$ V, along with the full Fano factor computed performing SC and SC-MC simulations. Remarkably, in this case a mode space approach taking into account all modes (i.e., 13) is mandatory in order to reproduce all cor-

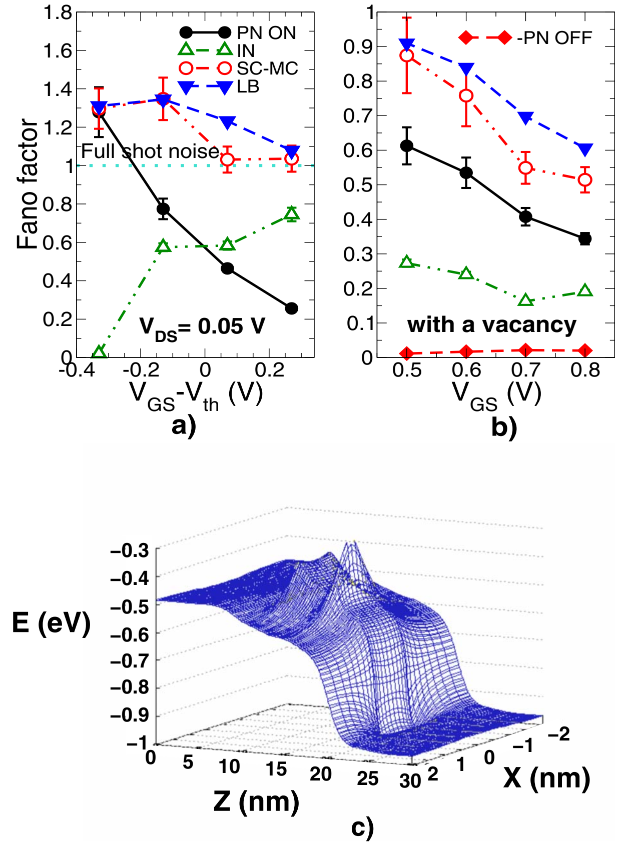

FIG. 6. (Color online) a) Contributions to the Fano factor F by the on-diagonal partition noise (solid circles), and the injection noise (open triangles up) as a function of the gate overdrive $V_{GS}-V_{th}$, for a drain-to-source bias $V_{DS}=50$ mV. The simulated device is a CNT-FET. The full noise computed by means of SC-MC simulations (open circles, both Pauli and Coulomb interactions taken into account) and applying Eq. (25) (solid triangles down, only Pauli exclusion considered) is also shown. b) Contributions to F by the on-diagonal and off-diagonal partition noise and by the injection noise [exploiting Eq. (18)] as a function of the gate overdrive for a CNT-FET with a vacancy in a site at the center of the channel. The drain-to-source bias is 0.5 V. c) Self-consistent midgap potential obtained by using the Fermi statistics for a gate voltage $V_{GS}=0.7$ V and a bias $V_{DS}=0.5$ V. Z is the transport direction along the channel, X is a transversal direction. The simulated device is the same of b).

relation effects on noise. As can be seen, off-diagonal exchange correlations gives rise to a not negligible correction to the Fano factor ($\approx 4\%$ of the full Fano factor at $V_{GS}=0.8$ V). We observe that such correlations are only established between transmitted electrons states [second term in Eq. (18)], while correlations between reflected and transmitted electron states [third term in Eq. (18)] are negligible since almost all electrons injected from the receiving contact D are reflected back because of the high bias condition. In this paper we have assumed phase-coherent quantum transport at room temperature. Our tools cannot include electron-phonon interaction, that a room temperature may play a role even in nanoscale devices. Reference 33 has considered the effect of electron-phonon scattering and has neglected Coulomb interaction: they find that electron-phonon scattering

increase shot noise in the above threshold regime, due to the broadening of the energy range of electron states contributing to transport.

V. CONCLUSION

We have developed a novel and general approach to study shot noise in ballistic quasi one-dimensional CNT-FETs and SNW-FETs. By means of a statistical approach within the second quantization formalism, we have shown that the Landauer-Büttiker noise formula [Eq. (25)] can be generalized to include also Coulomb repulsion among electrons. This point is crucial, since we have verified that by only using Landauer-Büttiker noise formula, i.e., considering only Pauli exclusion principle, one can overestimate shot noise by as much as 180%. From a computational point of view, we have quantitatively evaluated shot noise in CNT-FETs and SNW-FETs by self-consistently solving the electrostatics and the transport equations within the NEGF formalism, for a large ensemble of snapshots of device operation, each corresponding to a different configuration of the occupation of injected states.

Furthermore, with our approach we are able to observe a rectification of the dc characteristics due to fluctuations of the channel potential, and to identify and evaluate quantitatively the different contributions to shot noise. We are also able to consider the exchange interference effects, which are often negligible but can be measurable when a defect, introducing significant mode mixing, is inserted in the channel.

ACKNOWLEDGMENTS

The work was supported in part by the EC Seventh Framework Program under the Network of Excellence NANOSIL (Contract No. 216171), and by the European Science Foundation EUROCORES Program Fundamentals of Nanoelectronics, through funds from CNR and the EC Sixth Framework Program, under project DEWINT (Contract No. ERAS-CT-2003-980409). The authors would like to thank M. Büttiker for fruitful discussion.

APPENDIX

Let us consider a 2D channel of length L and denote with x and y the longitudinal direction and the transverse one, respectively. If the interface between the lead S (D) and the conductor is defined by $x_S=0(x_D=0)$, $\mathbf{G}_{DS}(y_D;y_S)=\mathbf{G}_{DS}(x_D=0,y_D;x_S=0,y_S)$ represents the wave function at $(x_D=0,y_D)$ due to an excitation at $(x_S=0,y_S)$. In real space the *Fisher-Lee relation* reads,

$$\mathbf{s}_{nm}=-\delta_{nm}+\frac{i\hbar\sqrt{v_n v_m}}{a}\int dy_D\int dy_S\chi_n(y_D)\mathbf{G}_{DS}(y_D;y_S)\chi_m(y_S), \tag{A.1}$$

where n is a mode outgoing at lead D with velocity v_n, m is a mode incoming at lead S with velocity v_m and a is the lattice constant along the x direction. In the **k**-representation, for a conductor of uniform cross-section, we can exploit a mode representation in the transverse direction and a plane wave representation in the longitudinal direction and Eq. (A.1) becomes

$$\mathbf{s}_{nm}=-\delta_{nm}+\frac{i\hbar\sqrt{v_n v_m}}{L}\mathbf{G}_{DS}(n,m), \tag{A.2}$$

where $\mathbf{G}_{DS}(n,m)=\mathbf{G}_{DS}(n,k_n;m,k_m)$ and k_n is the longitudinal wave vector of the transverse mode n. Let us assume both leads to be identical and denote with $\{k_1^S,\ldots,k_N^S\}(\{k_1^D,\ldots,k_N^D\})$ the set of wave vectors associated to the N modes coming from the lead S (D). Since the only nonzero components of the self-energy involve the end-points, in the **k**-representation $\mathbf{\Gamma}_S$ and $\mathbf{\Gamma}_D$ can be expressed as

$$\mathbf{\Gamma}_S=\begin{pmatrix}\mathbf{\Gamma}_{S;11} & \mathbf{0}\\ \mathbf{0} & \mathbf{0}\end{pmatrix}_{2N\times 2N}\qquad \mathbf{\Gamma}_D=\begin{pmatrix}\mathbf{0} & \mathbf{0}\\ \mathbf{0} & \mathbf{\Gamma}_{D;22}\end{pmatrix}_{2N\times 2N},$$

where $\mathbf{\Gamma}_{S;11}(n,m)=\delta_{nm}\frac{\hbar v(k_n^S)}{L}\,\forall\, n,m\in S$ and $\mathbf{\Gamma}_{D;22}(n,m)=\delta_{nm}\frac{\hbar v(k_n^D)}{L}\,\forall\, n,m\in D$.

Generalization to a CNT-FET structure is straightforward. Let us indicate with N_C and N_M the number of carbon atoms rings and the number of modes propagating along the channel, respectively. Since the coupling between the identical reservoirs and the channel involve only the end rings of the channel, $\mathbf{\Gamma}_S$ and $\mathbf{\Gamma}_D$ are $(N_M N_C)\times(N_M N_C)$ diagonal matrix and the only nonzero blocks are the first one and the latter one, respectively:

$$\mathbf{\Gamma}_{S;11}(n,m)=\delta_{nm}\frac{\hbar v(k_n)}{L}\quad \forall\, n,m=1,\cdots,N_M,$$

$$\mathbf{\Gamma}_{D;N_cN_c}(n,m)=\delta_{nm}\frac{\hbar v(k_n)}{L}\quad \forall\, n,m=1,\cdots,N_M. \tag{A.3}$$

By exploiting Eqs. (A.2) and (A.3) we can find the transmission ($\mathbf{t}$) and reflection ($\mathbf{r}$) amplitude matrix,

$$\mathbf{t}_{nm}=i\sqrt{\mathbf{\Gamma}_{D;N_CN_C}(n,n)}\mathbf{G}_{N_C1}(n,m)\sqrt{\mathbf{\Gamma}_{S;11}(m,m)},$$

$$\mathbf{r}_{nm}=-\delta_{nm}+i\sqrt{\mathbf{\Gamma}_{S;11}(n,n)}\mathbf{G}_{11}(n,m)\sqrt{\mathbf{\Gamma}_{S;11}(m,m)}. \tag{A.4}$$

Since at zero magnetic field $\mathbf{t}'=\mathbf{t}^{\mathbf{t}}$, relations Eq. (A.4) is all we need to compute the power spectral density Eq. (1) from Eq. (18). A similar procedure has been adopted for SNW-FETs where, from a computational point of view, the channel has been discretized in a sequence of slices in the longitudinal direction. In this case equations in Eq. (A.4) are obtained as well, but replacing the number of rings with the number of slices.

[1] R. Landauer, Nature (London) **392**, 658 (1998).
[2] Y. M. Lin, J. Appenzeller, J. Knoch, Z. Chen, and P. Avouris, Nano Lett. **6**, 930 (2006).
[3] J. Appenzeller, Y.-M. Lin, J. Knoch, Z. Chen, and P. Avouris, IEEE Trans. Nanotechnol. **6**, 368 (2007).
[4] J. Tersoff, Nano Lett. **7**, 194 (2007).
[5] P.-E. Roche, M. Kociak, S. Guéron, A. Kasumov, B. Reulet, and H. Bouchiat, Eur. Phys. J. B **28**, 217 (2002).
[6] L. G. Herrmann, T. Delattre, P. Morfin, J.-M. Berroir, B. Placais, D. C. Glattli, and T. Kontos, Phys. Rev. Lett. **99**, 156804 (2007).
[7] Y. Naveh, A. N. Korotkov, and K. K. Likharev, Phys. Rev. B **60**, R2169 (1999).
[8] G. Iannaccone, J. Comput. Electron. **3**, 199 (2004).
[9] G. Iannaccone, G. Lombardi, M. Macucci, and B. Pellegrini, Phys. Rev. Lett. **80**, 1054 (1998).
[10] G. Iannaccone, M. Macucci, and B. Pellegrini, Phys. Rev. B **55**, 4539 (1997).
[11] Y. M. Blanter and M. Buttiker, Phys. Rev. B **59**, 10217 (1999).
[12] O. M. Bulashenko and J. M. Rubí, Phys. Rev. B **64**, 045307 (2001).
[13] M. Büttiker, Phys. Rev. B **46**, 12485 (1992).
[14] T. Martin and R. Landauer, Phys. Rev. B **45**, 1742 (1992).
[15] S. Datta, Superlattices Microstruct. **28**, 253 (2000).
[16] A. van der Ziel, *Noise in Solid State Devices and Circuits* (Wiley, New York, 1986), pp. 16 and 75–78.
[17] Y. M. Blanter and M. Büttiker, Phys. Rep. **336**, 1 (2000).
[18] S. Datta, *Electronic Transport in Mesoscopic Systems* (Cambridge University Press, Cambridge, England, 1995).
[19] R. Landauer, IBM J. Res. Dev. **1**, 223 (1957).
[20] A. Betti, G. Fiori, and G. Iannaccone, IEEE Trans. Electron Devices **56**, 2137 (2009).
[21] N. Sai, M. Zwolak, G. Vignale, and M. Di Ventra, Phys. Rev. Lett. **94**, 186810 (2005).
[22] G. Vignale and M. Di Ventra, Phys. Rev. B **79**, 014201 (2009).
[23] Code and documentation can be found at the URL: http://www.nanohub.org/tools/vides, DOI: 10254/nanohub-r5116.3.
[24] A. Betti, G. Fiori, and G. Iannaccone, Tech. Dig. - Int. Electron Devices Meet. **1**, 185 (2008).
[25] D. S. Fisher and P. A. Lee, Phys. Rev. B **23**, 6851 (1981).
[26] G. Fiori and G. Iannaccone, IEEE Trans. Nanotechnol. **6**, 475 (2007).
[27] J. Guo, S. Datta, M. Lundstrom, and M. P. Anantam, Int. J. Multiscale Comp. Eng. **2**, 257 (2004).
[28] G. Fiori and G. Iannaccone, IEEE Trans. Nanotechnol. **6**, 524 (2007).
[29] J. Wang, E. Polizzi, and M. Lundstrom, J. Appl. Phys. **96**, 2192 (2004).
[30] T. Gramespacher and M. Büttiker, Phys. Rev. B **60**, 2375 (1999).
[31] E. V. Sukhorukov and D. Loss, Phys. Rev. Lett. **80**, 4959 (1998).
[32] M. Büttiker, Phys. Rev. Lett. **68**, 843 (1992).
[33] H. H. Park, S. Jin, Y. J. Park, and H. S. Min, J. Appl. Phys. **105**, 023712 (2009).